2015 International Symposium on Nonlinear Theory and its Applications
NOLTA2015, Kowloon, Hong Kong, China, December 1-4, 2015

RC Chaotic Oscillator Using Pulse Generator and Differ Amplifier

Yoshinori Doike†, Yoko Uwate†and Yoshifumi Nishio†

† Dept. of Electrical and Electronic Engineering, Tokushima University
2-1 Minamijosanjima, Tokushima, 770-8506 Japan
Email: {doike, uwate, nishio}@ee.tokushima-u.ac.jp

Abstract—In this study, a simple chaotic oscillator composed of RC phase shift oscillators using operational amplifier and pulse generator is proposed and investigated. By inputing pulse wave to operational amplifier of RC phase shift oscillator, chaotic phenomena are observed easily. We carry out computer calculation and circuit experiment in order to check the validity of the proposed model. And, we derive the one parameter bifurcation diagram.

1. Introduction

Recently, many researchers have taken an their interest in chaos [1][2]. Because, chaotic phenomena can be observed in various fields and chaotic systems are good models to explain and describe the higher dimensional nonlinear phenomena. In the field of electrical and electronic engineering, various applications based on deterministic chaos have been proposed [3][4]. For realizing such applications, we need chaotic oscillators.

There are various chaotic oscillators [5][6]. These oscillators are composed of RC circuits, pulse generators and operational amplifiers. By not using inductor, it can be easily integrated chaotic oscillators. When the parameters are varied, chaotic attractor are observed in this simple oscillator. However, it is not difficult to analyze these chaotic oscillators. These oscillators are pulse-driven non autonomous and discontinuous systems. When the output of pulse generators varies, operational amplifier's output varies. To analyze discontinuous system, it is necessary to follow complex procedures [7].

In this study, we propose new RC chaotic oscillator. The proposed model is composed of RC phase shift oscillators using operational amplifier and pulse generators. By inputing pulse wave to operational amplifier of RC phase shift oscillator, chaotic phenomena are observed easily. We carry out computer calculation and circuit experiment in order to check the validity of the proposed model. And, we derive the one parameter bifurcation diagram.

2. Circuit Model

Figure 1 shows the circuit model in this study. The proposed model is composed of RC phase shift oscillator with an operational amplifier and a pulse generator. The pulse wave is inputted to non-inverting input terminal of the operational amplifier. The differ amplifier produces the output voltage v_o which is their power supply voltage, according to the input signals.

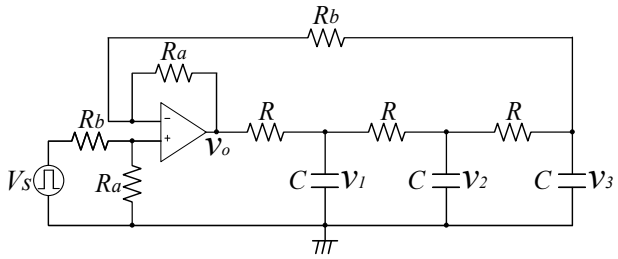

Figure 1: Circuit model.

Figures 2 shows the approximated $v_i - v_o$ characteristic of the deffer amplifier.

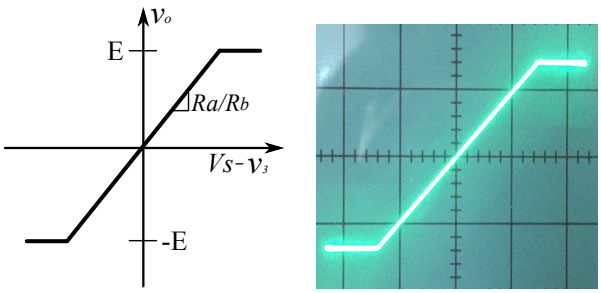

(a) (b)

Figure 2: Approximated $v_i - v_o$ characteristic of the deffer amplifier.

v_i corresponds to $V_S - v_3$. By using differ amplifiers, the proposed model has a continuity unlike using comparators. The differ amplifier's output varies smooth even though the output of pulse generators varies. The following equation of the approximated $v_i - v_o$ characteristic of the deffer amplifier is described as follows:

$$v_o = \frac{1}{2}\left\{|\frac{R_a}{R_b}(V_S - v_3) + E| - |\frac{R_a}{R_b}(V_S - v_3) - E|\right\}. \quad (1)$$

Figure 3(a) shows the input voltage waveform $V_S(t)$. V is the amplitude of the pulse voltage and T is the period of

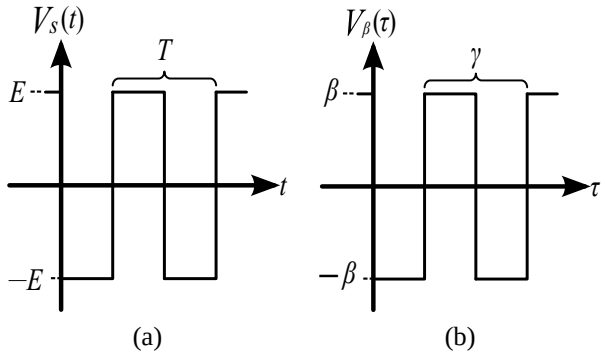

(a) (b)

Figure 3: Input voltage waveforms.

the waveform. Figure 3(b) shows the normalized voltage waveform $V_\beta(\tau)$. V_β corresponds to V_S, γ corresponds to T and τ corresponds to t.

The proposed model consists of only simple RC phase shift oscillators and a pulse generator. Namely, neither inductors nor negative resistors are included. Therefore, it is considered to be realized on the IC chip without complication.

The circuit equations are described as follows:

$$\begin{aligned} RC\frac{dv_1}{dt} &= -2v_1 + v_2 + v_o \\ RC\frac{dv_2}{dt} &= v_1 - 2v_2 + v_3 \\ RC\frac{dv_3}{dt} &= v_2 - v_3. \end{aligned} \tag{2}$$

By using the following variables and the parameters,

$$\begin{aligned} &v_1 = Ex,\ v_2 = Ey,\ v_3 = Ez,\ \frac{d}{dt} = \dot{} \\ &t = RC\tau,\ \alpha = \frac{R_a}{R_b},\ V_S = E\beta,\ T = RC\gamma, \end{aligned} \tag{3}$$

the normalized circuit equation is described as follows:

$$\begin{aligned} \dot{x} &= -2x + y + f(z) \\ \dot{y} &= x - 2y + z \\ \dot{z} &= y - z. \end{aligned} \tag{4}$$

where $f(z)$ is a piecewise-linear function corresponding to the $v_i - v_o$ characteristic of the deffer amplifier and is described as

$$f(z) = \frac{1}{2}\left\{|\alpha(\beta - z) + 1| - |\alpha(\beta - z) - 1|\right\}. \tag{5}$$

3. Exact Solutions

Since the circuit equations (4) are piecewise-linear, exact solutions in each linear region can be derived. At first, we define three piecewise-linear regions as follows:

$$\begin{aligned} &\mathbf{R_1} : \alpha(\beta - z) \le -1 \\ &\mathbf{R_2} : -1 < \alpha(\beta - z) < 1 \\ &\mathbf{R_3} : \alpha(\beta - z) \ge 1. \end{aligned} \tag{6}$$

Namely, $\mathbf{R_1}$ corresponds to the region where the output of differ amplifier is minimum values. On the other hand, $\mathbf{R_3}$ corresponds to the region where the output of differ amplifier is maximum values. And, $\mathbf{R_3}$ corresponds to the region where the output of differ amplifier is varied.

We calculate the eigenvalues in each region from Eq. (4). The eigenvalues in each region are described as follows,

$$\begin{aligned} &\mathbf{R_1} \text{ and } \mathbf{R_3} : \lambda_a, \lambda_b, \lambda_c \\ &\mathbf{R_2} : \lambda_2, \sigma_2 \pm j\omega_2. \end{aligned} \tag{7}$$

The eigenvalues of $\mathbf{R_1}$ and $\mathbf{R_3}$ can be derived from

$$\begin{vmatrix} \lambda + 2 & -1 & 0 \\ -1 & \lambda + 2 & -1 \\ 0 & -1 & \lambda + 1 \end{vmatrix} = 0. \tag{8}$$

On the other hand, the eigenvalues of $\mathbf{R_2}$ can be derived from

$$\begin{vmatrix} \lambda + 2 & -1 & \alpha \\ -1 & \lambda + 2 & -1 \\ 0 & -1 & \lambda + 1 \end{vmatrix} = 0. \tag{9}$$

Next, we define the equilibrium points in each regions as

$$\begin{aligned} \mathbf{E_1} &= [E_{11} \quad E_{12} \quad E_{13}]^{\mathrm{T}} \\ \mathbf{E_2} &= [E_{21} \quad E_{22} \quad E_{23}]^{\mathrm{T}} \\ \mathbf{E_3} &= [E_{31} \quad E_{32} \quad E_{33}]^{\mathrm{T}}, \end{aligned} \tag{10}$$

respectively. These values are calculated by putting right side of Eq. (4) to be equal to zero.

Then, we can described the exact solutions as follows. In $\mathbf{R_1}$ and $\mathbf{R_3}$:

$$\mathbf{x_a}(\tau) - \mathbf{E_n} = \mathbf{F}(\tau) \cdot \mathbf{F}^{-1}(0) \cdot (\mathbf{x_a}(0) - \mathbf{E_n}),$$

where

$$\begin{aligned} &\mathbf{x_a}(\tau) = [x_n(\tau) \quad y_n(\tau) \quad z_n(\tau)]^{\mathrm{T}}, \\ &\mathbf{F}(\tau) = [\mathbf{f_a}(\tau) \quad \mathbf{f_b}(\tau) \quad \mathbf{f_c}(\tau)]^{\mathrm{T}}, \\ &\mathbf{f_c}(\tau) = [\lambda_a \quad \lambda_b \quad \lambda_c], \\ &\mathbf{f_b}(\tau) = \frac{d\mathbf{f_c}(\tau)}{d\tau} + \mathbf{f_c}(\tau), \\ &\mathbf{f_a}(\tau) = \frac{d\mathbf{f_b}(\tau)}{d\tau} + \mathbf{f_b}(\tau). \end{aligned} \tag{11}$$

$(n = 1, 3)$

In $\mathbf{R_2}$:

$$\mathbf{x_b}(\tau) - \mathbf{E_2} = \mathbf{G}(\tau) \cdot \mathbf{G}^{-1}(0) \cdot (\mathbf{x_b}(0) - \mathbf{E_2}),$$

where

$$\mathbf{x_b}(\tau) = [x_2(\tau) \quad y_2(\tau) \quad z_2(\tau)]^{\mathrm{T}},$$
$$\mathbf{G}(\tau) = [\mathbf{g_a}(\tau) \quad \mathbf{g_b}(\tau) \quad \mathbf{g_c}(\tau)]^{\mathrm{T}},$$
$$\mathbf{g_c}(\tau) = [\mathrm{e}^{\lambda_2\tau} \quad \mathrm{e}^{\sigma_2\tau}\cos\omega_2\tau \quad \mathrm{e}^{\sigma_2\tau}\sin\omega_2\tau]^{\mathrm{T}},$$
$$\mathbf{g_b}(\tau) = \frac{d\mathbf{g_c}(\tau)}{d\tau} + \mathbf{g_c}(\tau),$$
$$\mathbf{g_a}(\tau) = \frac{d\mathbf{g_b}(\tau)}{d\tau} + \mathbf{g_b}(\tau). \tag{12}$$

4. Results

We show the chaotic attractors which are obtained by computer calculation and circuit experiment as shown Fig. 4.

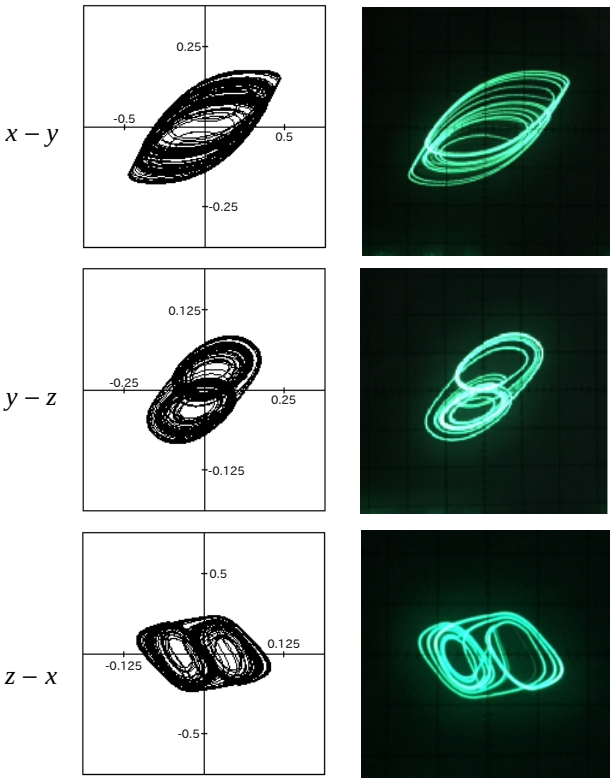

Figure 4: The chaotic attractors obtained from the proposed model. (1) Computer calculation. ($\alpha = 50, \beta = 0.03$, and $\gamma = 7.3$) (2) Circuit Experiment. ($R = 10[k\Omega], R_a = 750[k\Omega], R_b = 15[k\Omega], C = 103[nF], V_S = 0.3[V]$ and $f = 140[Hz]$)

We can observed almost same attractors. The attractors of RC chaotic oscillator which consists in a pulse generator are angular[5][6]. On the other hand, the attractors of the proposed model are round.

In order to confirm the generation of chaos and to investigate bifurcation scenario, we derive the Poincare map.

Let us define the following subspace

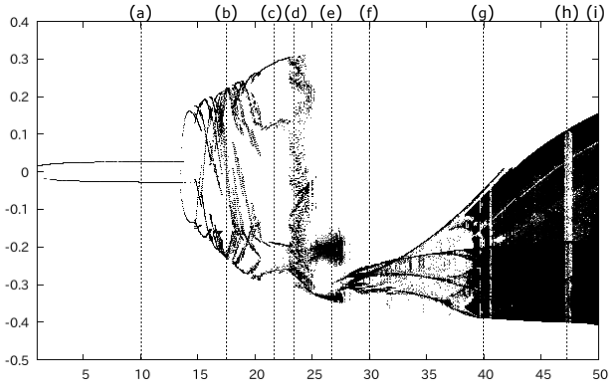

Figure 5: One parameter bifurcation diagram when α is varied.

$$\mathbf{S} = \mathbf{S_1} \cap \mathbf{S_2}, \tag{13}$$

where

$$\mathbf{S_1} : \beta > 0$$
$$\mathbf{S_2} : \tau = n\gamma \qquad (n = 1, 2, 3, ...). \tag{14}$$

The subspace $\mathbf{S_1}$ shows that the output of pulse generator is maximum, while the subspace $\mathbf{S_2}$ shows that the output of pulse generator varies. Namely, $\mathbf{S}$ corresponds to the transitional condition from $-\beta$ to β.

We chose α as the control parameter and other parameters are fixed as $\beta = 0.03, \gamma = 7.3$.

Figure 5 shows the one parameter bifurcation diagram when α is varied from 1 to 50. The vertical axis shows x_1, the horizontal axis shows α, parameter step is 0.001 and plotted point is $1000[\tau]$. And, Figures 6 show the attractors of computer calculation.

For $1 < \alpha < 14.29$, the oscillation is not observed from Fig. 6(a) and the values vary depending on the initial values. From these results, we can observe the periodic orbits, torus and chaotic phenomena. In particular, we focus on the chaotic phenomena when α is 23.83 and 50. In order to compare two types chaotic phenomena, we show the Poincare maps and the largest Lyapunpv exponents when α is 23.83 and 50. The largest Lyapunov exponents are given by

$$\mu = \frac{1}{n}\lim_{n\to\infty}\sum_{k=1}^{n} log2\,\frac{x_1(\tau+\gamma)}{x_1(\tau)}. \tag{15}$$

Table 1: Comparative results.

α	Lyapunov exponent	Transitional condition
22.83	0.000594	Continuity
50	0.000818	Discontinuity

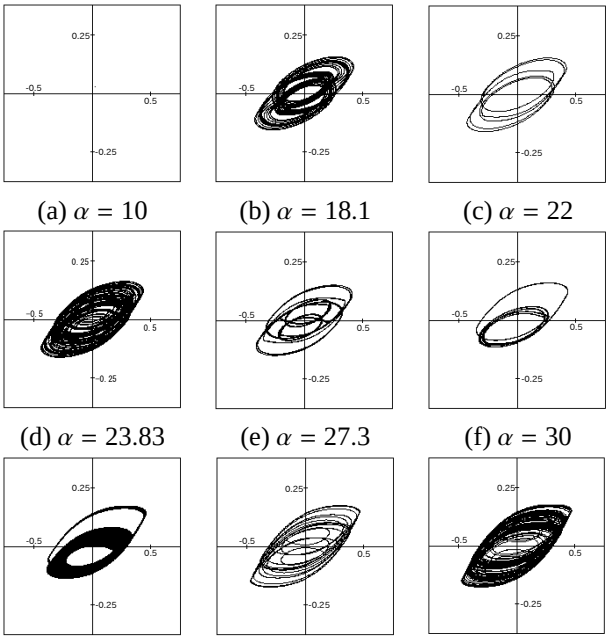

(a) α = 10 (b) α = 18.1 (c) α = 22

(d) α = 23.83 (e) α = 27.3 (f) α = 30

(g) α = 40 (h) α = 47.3 (i) α = 50

Figure 6: Computer calculated results.

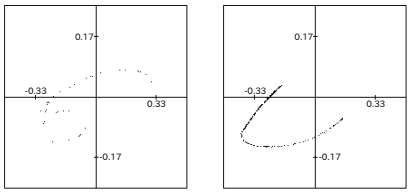

α = 23.83 α = 50

Figure 7: The Poincare maps.

From Fig. 7, it is seen that two types chaotic attractors are different. In case that α is 50, piecewise-linear regions is changed from $\mathbf{R_1}$ to $\mathbf{R_3}$ or $\mathbf{R_3}$ to $\mathbf{R_1}$. Namely, discontinuity is observed on the proposed model. Almost RC chaotic oscillators containing pulse generator have discontinuity. On the other hand, in case that α is 23.83, discontinuity is not observed. By using differ amplifier, piecewise-linear regions is changed smoothly. Therefore, continuity is observed on the proposed model.

5. Conclusion

In this study, we have investigated a RC chaotic oscillator. The proposed model is composed of RC phase shift oscillator with an operational amplifier and a pulse generator. By inputing pulse wave to operational amplifier of RC phase shift oscillator, chaotic phenomena are observed easily. We have carried out computer calculation and circuit experiment to investigate. From computer calculations and circuit experiments, we have checked the validity of the proposed model. And, we have observed the periodic orbits, torus and chaotic phenomena. Moreover, we have observed two types chaotic phenomena. The one is chaotic phenomena with discontinuity. The other is chaotic phenomena with continuity in spite of using pulse generator.

In our future works, we will derive the Lyapunov exponents by using Jacobian in order to investigate the proposed model in detail. And, we will investigate the correlations of between chaotic phenomena and other parameters.

References

[1] S. Vlad, P. Pascu and N. Moraiu, “Chaos Models in Economics,” Journal of Computing, vol. 2, Issue 1, pp. 79-83, January, 2010.

[2] J. E. Skinner, M. Molnar, T. Vybiral and M. Mitra, “Application of Chaos Theory to Biology and Medicine,” Integrative Physiological and Behavioral Science, vol. 27, Issue 1, pp. 39-53, January-March, 1992.

[3] K. Aihara, “Chaos Engineering and Its Applications to Parallel Distributed Processing with Chaotic Neural Networks,” Proc. of IEEE 90.5, pp. 919-930, May, 2002.

[4] K. M. Cuomo, A. V. Oppenheim and S. H. Strogatz, “Synchronization of Lorenz-based Chaotic Circuits with Applications to Communications,” IEEE Trans. Circuits and Systems, vol.40, no.10, pp, pp. 626-633, October, 1993.

[5] A. S. Elwakil and S. Ozoguz, “Pulse-excited RC Nonautonomous Chaotic Oscillator Structures,” Journal of Bifurcation and Chaos, vol. 15, no. 7, pp. 2257-2261, August, 2005.

[6] S. Masuda, Y. Uchitani, and Y. Nishio, “Simple Chaotic Oscillator Using Two RC Circuits,” Proc. of NCSP’09, pp. 89-92, March, 2009.

[7] R. I. Leine, D. H. Van Campen, and B. L. Van De Vrande, “Bifurcations in Nonlinear Discontinuous Systems,” Nonlinear dynamics, vol. 23, Issue. 2, pp. 105-164, October, 2000.